Published in final edited form as:

Mod Pathol. 2020 September ; 33(9): 1669–1677. doi:10.1038/s41379-020-0557-5.

Undifferentiated Round Cell Sarcoma with *BCOR* Internal Tandem Duplications (ITD) or *YWHAE* fusions: A Clinicopathologic and Molecular Study

Cristina R Antonescu, MD[1], **Yu-Chien Kao, MD**[2], **Bin Xu, MD**[1], **Yumi Fujisawa**[1], **Catherine Chung, MD**[3], **Christopher D.M. Fletcher, MD**[4], **Nicole Graf, MD**[5], **Albert J. Suurmeijer, MD**[6], **Angelica Zin, PhD**[7], **Leonard H Wexler, MD**[8], **Andrea Ferrari, MD**[9], **Gianni Bisogno, MD**[10], **Rita Alaggio, MD**[11]

[1]Department of Pathology, Memorial Sloan Kettering Cancer Center, New York, NY [2]Department of Pathology, Shuang Ho Hospital, Taipei Medical University, Taipei, Taiwan [3]Department of Pediatric Laboratory Medicine, The Hospital for Sick Children, Toronto, Canada [4]Department of Pathology, Brigham and Women's Hospital, Boston, MA [5]Department of Histopathology, University of Sydney, The Children's Hospital at Westmead, Sydney, New South Wales, Australia [6]Department of Pathology and Medical Biology, University Medical Center Groningen, University of Groningen, Groningen, The Netherlands [7]Institute of Pediatric Research Città della Speranza, Padova, Italy [8]Department of Pediatrics, Memorial Sloan Kettering Cancer Center, New York, NY [9]Pediatric Oncology Unit, Fondazione IRCCS Istituto Nazionale dei Tumori, Milan, Italy [10]Department of Pediatric Hematology-Oncology, University of Padova, Padova, Italy [11]Department of Pathology, Hospital Bambino Gesu, Rome, Italy

Abstract

Until recently, undifferentiated round cell sarcomas (URCS) in infants have been considered a wastebasket diagnosis, composed of various pathologic entities and lacking consistent genetic alterations. The recent identification of recurrent *BCOR* internal tandem duplications (ITD) and less common alternative *YWHAE-NUTM2B/E* fusions in half of infantile URCS and the majority of so-called primitive myxoid mesenchymal tumors of infancy (PMMTI) suggests a common pathogenesis with clear cell sarcoma of the kidney which also harbors the same genetic alterations. These tumors also share a similar morphology and immunoprofile, including positivity for BCOR, cyclin D1 and SATB2. In this study we investigate the largest cohort to date of genetically confirmed URCS and PMMTI with *BCOR* ITD or *YWHAE* fusions to better define their morphologic spectrum and clinical behavior. Twenty-eight cases harbored *BCOR* ITD and 5 *YWHAE* fusions, occurring in 29 infants and 4 children, 19 males and 14 females.

Correspondence: Cristina Antonescu, MD, Department of Pathology, Memorial Sloan-Kettering Cancer Center, 1275 York Ave, New York 10065; antonesc@mskcc.org.

Conflicts of Interest: The authors declare no conflicts of interest

Data Availability Statement: The data that support the findings of this study are available from the corresponding author upon reasonable request.

Microscopically, 20 were classified as URCSs and 13 as PMMTI. Follow-up was available in 25 patients, with 14 (56%) succumbing to their diseases at a mean duration of 18-months follow-up (range: 2–62). Six patients remained with no evidence of disease at a mean follow-up of 63 months (range: 4–192), 4 patients were still alive with disease (mean follow-up: 46 months, range: 4–120), and 1 died of other causes. Local recurrence and distant metastasis were each observed in 11/25 (44%) of the patients. The overall survival was 42% at 3 years and 34% at 5 years (median survival: 26 months). There was no statistically significant survival difference between cases diagnosed as URCS and PMMTI and between those with BCOR ITD and YWHAE fusions.

Keywords

BCOR; *YWHAE*; undifferentiated round cell sarcoma; PMMTI

INTRODUCTION

The BCOR family of tumors includes a number of different entities, including soft tissue undifferentiated round cell sarcomas (URCS), primitive myxoid mesenchymal tumors of infancy (PMMTI), clear cell sarcoma of kidney (CCSK), and certain uterine sarcomas and intracranial tumors, having in common an undifferentiated round to spindle cell phenotype and overexpression of BCOR at both mRNA and protein levels. The *BCOR* genetic abnormalities include either ITD or various *BCOR* fusions, more often involving the *CCNB3* gene and less commonly other partners[1–3]. In a small subset of cases, alternative *YWHAE-NUTM2B/E* fusions may substitute for *BCOR* ITD as the driver oncogenic event[4]. Despite their significant morphologic and immunohistochemical overlap, the BCOR family of tumors comprise pathologic entities showing distinctive clinical presentations. For example, *BCOR* ITD-positive URCS and PMMTI are often limited to infants and truncal or intra-abdominal soft tissue sites, while CCSK involves the kidney of young children (2–4 years old), and tumors harboring *BCOR-CCNB3* fusions occur with predilection in the skeleton of adolescents[1,2]. While the clinical behavior of CCSKs and *BCOR-CCNB3*-positive sarcomas have been studied in larger series[1,5], the prognosis of *BCOR* ITD-positive URCS/PMMTI has not yet been established. Furthermore, it remains unclear if any morphologic or genotypic parameters are predictive of patient outcome. In this study, we investigate the pathologic features and clinical behavior of a large cohort of genetically confirmed *BCOR* ITD/ *YWHAE-NUTM2B/E*-positive URCS and PMMTI.

MATERIALS AND METHODS

Patient Selection and Histologic Diagnosis

Archival material from pediatric patients with diagnosis of either URCS or PMMTI, with confirmed molecular abnormalities of either *BCOR* ITD or *YWHAE-NUTM2B/E* fusions, was retrieved from the pathology files and personal consultations of the senior authors (CRA, CDF, RA) covering almost two decades (2001–2019). All cases were reviewed centrally at MSKCC, by two sarcoma pathologists CRA and YCK. The cases were identified mainly by morphology and patient age, and subsequently confirmed by molecular testing. Thirty-three cases were collected. Hematoxylin and eosin-stained tissue sections and

immunohistochemical stains (BCOR, SATB2) were available for re-review on all the cases selected for the study. Seventeen cases were previously included in the study by Kao YC et al., which reported follow-up data of only 7 cases available at that time.[4] In this study, we collected follow-up information of 14 of the 17 prior cases and also 11 of 16 subsequent cases. A diagnosis of PMMTI was designated if a sizable portion of the lesion was myxoid, arbitrarily designated as 30%, as no cutoff value was used in the initial description of PMMTI. However, most of the cases diagnosed as PMMTI in this series showed predominantly low cellularity, with the myxoid component often in the range of >80–90% of the material reviewed (Table 1). In all except two cases the material available for review was from the surgical resection. Clinical follow-up and detailed treatment information were obtained by reviewing the patients' charts. The study was approved by the Institutional Review Board at participating Institutions.

Molecular Testing Methods

Molecular tests were performed either retrospectively during our previous study (17 reported cases) or as part of the diagnostic workup (the remaining 16 cases). *BCOR* ITD was detected primarily by polymerase chain reaction (PCR), and in some cases also by whole transcriptome sequencing, and/or targeted sequencing methods, whereas *YWHAE* fusions were identified by fluorescence in situ hybridization (FISH) in all 5 cases, with some of them also detected by conventional cytogenetics, whole transcriptome sequencing, and/or reverse transcription-PCR (RT-PCR).

Whole transcriptome sequencing was performed in 7 cases using frozen tissue material, as previously reported.[4] Targeted sequencing was performed in 3 additional cases using one of the following panels: Archer DX, targeted exome and Foundation One (one case each). PCR and Sanger sequencing for *BCOR* ITD were performed using genomic DNA isolated either from fresh-frozen or archival paraffin tissue in 25 samples. The sequencing results of the PCR products were analyzed by comparing to the NCBI human *BCOR* gene sequences. FISH for *YWHAE* and *NUTM2B/E* break-apart gene abnormalities was performed using custom design bacterial artificial chromosome (BAC) probes. Two cases were further confirmed by RT-PCR for *YWHAE-NUTM2B* fusion. Conventional karyotyping was performed in two cases. The whole transcriptome sequencing method, PCR and RT-PCR primers and protocols, and BAC clones for FISH have been described previously.[4]

Statistical analysis

Statistical analysis was performed on SPSS software 22.0 (IBM Corporation, New York, NY, U.S.). The associations between the clinical variables and matched groups were evaluated by Fisher's exact test. The overall survival time was measured in months from the date of diagnosis to the date of death. Kaplan-Meier estimate was used to calculate the overall survival. The statistical significance of different pathologic and molecular variables, such as type of genetic alterations and the morphologic patterns, were assessed in relation to survival was assessed by log-rank analysis. Prognostic variables that were significant on univariate analyses were subsequently subjected to multivariate analyses using the Cox proportional hazards model. A $p<0.05$ was considered as significant for all statistical analyses.

RESULTS

Clinical Features

The clinicopathologic features are summarized in Table 1. All except four patients were infants (< 1 year of age), with 4 being diagnosed within the first month after birth, in keeping with congenital tumors. Two patients were diagnosed before age of 2, one of them presenting with a brain tumor. The remaining two patients were male teenagers, a 16 and a 17 year-old, both presenting with bone lesions, initially diagnosed as a small cell osteosarcoma due to the presence of tumoral mineralization observed radiographically. The entire cohort included 14 females and 19 males. Most tumors were located in the axial soft tissue, including trunk (back, paraspinal, intraspinal L1–5, flank, abdominal wall, chest wall; n=14), abdomen/retroperitoneum/pelvis (n=10) and intra-thoracic (n=2). Less frequent sites of involvement included 4 in the head and neck (larynx, jaw, neck, orbit), 2 central nervous system (1 intra-cranial/extra-axial, 1 posterior fossa) and 1 in the lower limb (ankle). Tumor size was available in 7 patients and varied from 2.5–13 cm (mean 7 cm).

Follow-Up and Survival Analysis

Follow-up information and treatment modalities were available in all except 8 patients, which were either very recent cases or lost during follow-up. Eleven patients (44%) each developed local recurrences and distant metastases (locoregional lymph nodes, brain and bone). At last follow-up, 14 patients died of the disease (56%). Eight of them died within the first year after diagnosis, and 5 of them between 2 to 5 years after diagnosis (mean: 18 months, range: 2–62 months). Another patient (case 26) with a primary ankle tumor, metastatic to the ipsilateral tibia and inguinal lymph node, was treated with amputation and chemotherapy, and succumbed of an episode of adenovirus hepatitis. The remaining 10 patients were still alive. Six of them had no evidence of disease (follow-up duration: 4–192 months, mean: 63 months), and 4 patients were alive with local or metastatic diseases (follow-up duration: 4–120 months, mean: 46 months).

All patients with primary tumors in the abdominal/pelvic cavity or retroperitoneum and with available follow-up information died of disease (100%, n=6), compared to 4 of 11 (36%) patients with tumors localized in the trunk. Most of the patients with no evidence of disease had the primary tumor located in the trunk (2 paraspinal, and 1 each in back, flank, chest wall and intraspinal L1–5).

All patients with information data available received chemotherapy in either the neoadjuvant or adjuvant setting (Table 1). Various chemotherapy regimens were administered. First-line chemotherapy consisted of the vincristine-actinomycin-D (VA) combination, as given for infantile fibrosarcoma, in 3 cases, subsequently followed by ifosfamide-based chemotherapy, i.e. ifosfamide-doxorubicin (ID) or ifosfamide-vincristine-actinomycin-D (IVA). One case received methotrexate, adriamycin and cisplatin (MAP). In all other cases, first-line chemotherapy included an alkylating agent – ifosfamide or cyclophosphamide – plus other drugs such as vincristine, actinomycin-D, doxorubicin, etoposide, or carboplatin, according to different regimens.

Treatment response to chemotherapy was available in 5 cases. Objective response was observed in two cases: one case with a flank tumor had >50% necrosis on histologic evaluation of the resection, performed after ifosfamide-based chemotherapy (case 3); the patient was alive and disease free at the time of the analysis, 16 years after diagnosis. The second responding patient had a 90% size reduction of a pre-sacral tumor after neoadjuvant multi-agent chemotherapy (case 13); however, the patient developed multiple brain metastases shortly after surgery and died of disease. Two other patients did not show any response to neoadjuvant chemotherapy (cases 6 and 25), while another (case 28) with a retroperitoneal/intra-abdominal tumor progressed on treatment.

The median follow-up time for survivors was 50 months (range 4–192 months). Overall survival for the entire cohort was 42% at 3 years and 34% at 5 years, respectively, with a median survival of 26 months. Of tumors with URCS histology, 11/16 (69%) patients died of the disease, while 3 of 9 (33%) PMMTI patients succumbed of the disease. The mortality rates were similar between patients with *YWHAE-NUTM2B/E* fusions (2/4, 50%) and those with *BCOR* ITD (12/21, 57%). Patients classified as PMMTI had a 5 year-survival rate of 45%, while the URCS 32%, however, the difference was not statistically significant (p=0.694; Fig 3A). Similarly, patients with *YWHAE*-positive tumors had a better outcome with a 5-year overall survival of 50%, compared to patients with *BCOR* ITD tumors, but was also not statistically significant (p=0.533; Fig 3B).

Pathologic Findings

Microscopic features revealed that 20 cases were predominantly solid and composed of sheets of primitive small blue round to ovoid cells arranged in vague nests separated by thin fibrous stroma (Fig. 1). Lesional cells typically showed scant palely eosinophilic cytoplasm and uniform round nuclei with fine chromatin. Except for two cases, all tumors showed high mitotic activity (>10 MF/10 HPFs) and often large areas of geographic necrosis. Most tumors showed a primitive round, ovoid or short spindle cell phenotype, while other patterns such as epithelioid with moderate to abundant cytoplasm or marked nuclear pleomorphism were typically absent. Some tumors showed perivascular condensation of the tumor cells and vague marbling, reminiscent of a high-grade malignant peripheral nerve sheath tumor (Fig. 1). Two cases occurring in the skeleton were associated with bone matrix, mostly in the form of reactive new bone formation and focally suggestive of osteoid deposition, leading to a misdiagnosis of osteosarcoma (Fig. 1). No morphologic differences were observed between tumors harboring *YWHAE* fusion or *BCOR* ITD.

Thirteen cases showed primitive round to ovoid cells embedded within an abundant myxoid stroma, in keeping with a diagnosis of PMMTI (Fig 2). Predominantly myxoid tumors had a deceptively bland and hypocellular appearance suggesting benign or low-grade diagnoses. A delicate vascular network was often noted. At higher magnification, the tumor cells showed round to ovoid nuclei, with mild to moderate atypia and diffuse hyperchromasia. Necrosis was present in a subset of cases, typically as a focal finding. Mitotic activity in this subset of cases was quite variable, ranging from 1–10 MF/10 HPFs.

All tumors showed diffuse and strong immunoreactivity for BCOR and SATB2, as previously reported (Figs. 1–2)[6]. A smaller subset (30%) of cases was also tested with cyclin

D1, which showed nuclear positivity. No other consistent marker expression was noted, most tumors being negative for desmin, myogenin, S100, SOX10, CK, etc. One case showed TLE1 strong positivity, while all cases tested with H3K27me3 showed retained expression.

Molecular Abnormalities

Five cases showed the presence of *YWHAE* gene rearrangements, with 4 cases being confirmed to have *YWHAE-NUTM2B/E* fusions (Table 1). In 2 of these cases, karyotype analysis was performed showing a balanced t(10;17) translocation in one case and a three-way translocation t(10;14;17) in a second. One case was studied by whole transcriptome analysis. The fusions were confirmed by FISH and/or RT-PCR. The other 2 were detected by FISH to have *YWHAE* gene rearrangements, including one with also *NUTM2B/E* rearrangement by FISH.

In the remaining 28 cases the presence of a *BCOR* ITD was confirmed by one or two different platforms as follows: genomic PCR and Sanger sequencing in 25 cases, whole transcriptome in 6 cases and various targeted RNA or DNA sequencing approaches in 3 cases (Table 1). The exact length of the ITD was determined in 21 cases, ranging from 63–129 base-pairs (bp), with the 2 most prevalent sizes being 66 and 96 bp.

DISCUSSION

Several groups of primitive round cell sarcomas are characterized by recurrent *BCOR* genetic alterations, resulting in oncogenic activation of *BCOR*. Although these pathologic entities show distinctive clinical presentations, they share significant overlap with regards to morphology, immunoprofile and molecular findings, suggesting a shared pathogenesis. The most common abnormality is a paracentric Xp11.4. inversion resulting in *BCOR-CCNB3* gene fusion, while less frequent examples harbor inter-chromosomal fusions between *BCOR* and various partners such as *MAML3, ZC3H7B, KMT2D, CHD9*, etc [1–3,7]. Although the *BCOR* breakpoints in the more prevalent *BCOR-CCNB3* and *BCOR-MAML3* fusions are consistently located in the last *BCOR* exon 15, encoding for the PUFD domain, the remaining *BCOR* fusion variants have variable breakpoints outside the PUFD domain[7]. In some of these fusions, *BCOR* has been reported as both the 5’ and 3’ partners; in the latter variants often lacking the typical BCOR overexpression[3,7]. Similar to *BCOR-CCNB3* fusions, ITD alterations occur consistently within the last exon of *BCOR*[4,5]. *BCOR* ITD have been described in half of the infantile URCS and in most PMMTI[4]. Rare cases of URCS harbor alternative *YWHAE-NUTMB/E* fusions resulting in a similar *BCOR* activation program[4]. Of interest, similar exon 15 *BCOR* ITD have also been described in a group of central nervous system primitive neuroectodermal tumors (CNS-PNET), similarly occurring in very young children[8], as well as in a rare subset of high grade endometrial stromal sarcomas with predominantly round cell morphology[9].

Primitive mesenchymal tumor of infancy (PMMTI) was initially described as a new category of pediatric fibroblastic-myofibroblastic tumors, distinct from congenital/infantile fibrosarcoma.[10] PMMTIs are characterized by variable cellularity ranging from hypocellular myxoid areas to sheets of primitive cells with spindle, polygonal, or round cytomorphology, within a myxoid matrix with delicate vasculature. However, no myxoid component cutoff

was used by the authors to define this entity. In this initial report, all 6 PMMTI occurred in infants, 3 of whom had congenital presentation of a soft tissue mass. Due to the overlapping clinical presentation in infants with the *BCOR* URCS, our initial study has investigated 7 such PMMTI cases, including 2 patients from the initial publication, and confirmed that that all except one case harbor similar *BCOR* ITD genetic alterations as demonstrated either by whole transcriptome or by genomic PCR[4]. In the current study, the 13 PMMTI cases were defined by the presence of a sizable myxoid component, arbitrarily, using arbitrarily a ≥30% myxoid component cut-off, although most cases were predominantly myxoid (>90%), with the primitive round to ovoid cells being embedded in a copious myxoid matrix. Of note, a small subset of URCS also showed focal areas of myxoid change, suggesting a likely morphologic spectrum. Moreover, there was no difference in the size of *BCOR* ITD alterations between URCS and PMMTI. However, 69% (11/16) patients with tumors displaying URCS histology died of disease, in contrast to 33% (3/9) PMMTI patients. Although both PMMTI histology and *YWHAE* fusions were associated with a better overall survival compared to URCS and *BCOR* ITD genetic abnormalities, the difference was not statistically significant, suggesting that these tumors belong to a single clinicopathologic entity and PMMTI likely represents a morphologic variant of URCS with *BCOR* ITD, similar to the wide histologic spectrum observed in CCSK.

Additional multi-institutional, larger studies are needed to evaluate the impact of these various histologic subtypes and their myxoid component with survival. Due to its rare incidence, most of the cases included in this current analysis represent outside consults, with the inherent limitation that not all the material was available for review, and thus the estimate of the myxoid component might be inaccurate due to sampling variability. Moreover, based on the experience learned from CCSK, no significant difference in their clinical outcome has been established based on histologic patterns[11]. Thus, the mere presence or absence of myxoid stroma may not justify subclassification of an entity, which otherwise shares similar clinical and genetic features. Interestingly, all 13 PMMTI harbored *BCOR* ITD, and none of the *YWHAE* fusion positive tumors were classified as PMMTI.

This is the first study evaluating the clinical behavior and the therapeutic strategies applied in these patients with either *BCOR* ITD or *YWHAE* fusions. Overall, among the 25 patients with available follow-up, 14 (56%) succumbed of their disease at a mean of 18 months follow-up, regardless of their morphologic appearance or genotype. Six patients remained with no evidence of disease at a mean follow-up of 63 months, two of them harbored a *YWHAE-NUTM2B/E* fusion and two displayed PMMTI histology. Our results demonstrated that patients followed a highly aggressive clinical course, with a 3-year overall survival of 42% and 5-year overall survival of 34% (median survival: 26 months). As a retrospective study of an extremely rare disease entity and a predominantly consultation-based case cohort, this study was bound to significant limitations, including small case number, lack of complete data on certain parameters, such as tumor size, disease stage at presentation, and margin status of surgical resection, and uniform therapy protocols. Further multi-institutional investigations or prospectively-driven case registry studies are needed to provide stronger correlations between pathologic findings and survival, and therefore to better guide treatments for these patients.

As previously documented, most of the patients were infants and presented with large, bulky tumors often involving the trunk or abdominal/pelvic cavity. Two outlier cases presented in older children (both male teenagers) as destructive and sclerotic bone tumors (vertebral body and scapula). Due to their radiographic appearance, focal bone matrix deposition and SATB2 diffuse reactivity, both cases were misinterpreted as small cell osteosarcomas and treated as such. The clinical features of these two cases (skeletal lesions in male children) is highly reminiscent of the common presentation of *BCOR-CCNB3* fusion positive sarcomas[1,2]. In fact, focal osteoid matrix deposition has been reported in rare cases of *BCOR-CCBN3* positive tumors, further highlighting diagnostic challenges[2].

In conclusion, this study investigated the clinicopathologic features of 33 patients with URCS harboring *BCOR* ITD or *YWHAE* fusion, with follow-up information in 25 of the cases, highlighting their aggressive clinical behavior. There was no significant survival difference between different genotypes (*BCOR* ITD vs *YWHAE* fusion) and between those classified microscopically as URCS and PMMTI, suggesting a single pathologic entity.

Acknowledgement

Dr. Matthew Drake, Canterbury Health Laboratories, Christchurch, New Zealand (Case 13).

Supported by: P50 CA140146–01 (CRA), P30 CA008748 (CRA), P50 CA217694 (CRA), Cycle for Survival (LW, CRA), St Baldrick Foundation (CRA), Kristen Ann Carr Foundation (CRA).

REFERENCES

1. Pierron G, Tirode F, Lucchesi C, Reynaud S, Ballet S, Cohen-Gogo S, et al. A new subtype of bone sarcoma defined by BCOR-CCNB3 gene fusion. Nat Genet. 2012;44:461–466. [PubMed: 22387997]
2. Kao YC, Owosho AA, Sung YS, Zhang L, Fujisawa Y, Lee JC, et al. BCOR-CCNB3 Fusion Positive Sarcomas: A Clinicopathologic and Molecular Analysis of 36 Cases With Comparison to Morphologic Spectrum and Clinical Behavior of Other Round Cell Sarcomas. Am J Surg Pathol. 2018;42:604–615. [PubMed: 29300189]
3. Specht K, Zhang L, Sung YS, Nucci M, Dry S, Vaiyapuri S, et al. Novel BCOR-MAML3 and ZC3H7B-BCOR Gene Fusions in Undifferentiated Small Blue Round Cell Sarcomas. Am J Surg Pathol. 2016;40:433–442. [PubMed: 26752546]
4. Kao YC, Sung YS, Zhang L, Huang SC, Argani P, Chung CT, et al. Recurrent BCOR Internal Tandem Duplication and YWHAE-NUTM2B Fusions in Soft Tissue Undifferentiated Round Cell Sarcoma of Infancy: Overlapping Genetic Features With Clear Cell Sarcoma of Kidney. Am J Surg Pathol. 2016;40:1009–1020. [PubMed: 26945340]
5. Roy A, Kumar V, Zorman B, Fang E, Haines KM, Doddapaneni H, et al. Recurrent internal tandem duplications of BCOR in clear cell sarcoma of the kidney. Nature Communications. 2015;6:8891.
6. Kao YC, Sung YS, Zhang L, Jungbluth AA, Huang SC, Argani P, et al. BCOR Overexpression is a Highly Sensitive Marker in Round Cell Sarcomas with BCOR Genetic Abnormalities. Am J Surg Pathol. 2016;40:1670–1678. [PubMed: 27428733]
7. Kao Y, Sung YS, Argani P, Swanson D, Alaggio R, Tap W, et al. Mod Pathol. 2020 [In Press].
8. Sturm D, Orr BA, Toprak UH, Hovestadt V, Jones DTW, Capper D, et al. New Brain Tumor Entities Emerge from Molecular Classification of CNS-PNETs. Cell. 2016;164:1060–1072. [PubMed: 26919435]
9. Marino-Enriquez A, Lauria A, Przybyl J, Ng TL, Kowalewska M, Debiec-Rychter M, et al. BCOR Internal Tandem Duplication in High-grade Uterine Sarcomas. Am J Surg Pathol 2018;42:335–341. [PubMed: 29200103]

10. Alaggio R, Ninfo V, Rosolen A, Coffin CM. Primitive myxoid mesenchymal tumor of infancy: a clinicopathologic report of 6 cases. Am J Surg Pathol. 2006;30:388–394. [PubMed: 16538060]
11. Argani P, Perlman EJ, Breslow NE, Browning NG, Green DM, D'Angio GJ, et al. Clear cell sarcoma of the kidney: a review of 351 cases from the National Wilms Tumor Study Group Pathology Center. Am J Surg Pathol. 2000;24:4–18. [PubMed: 10632483]

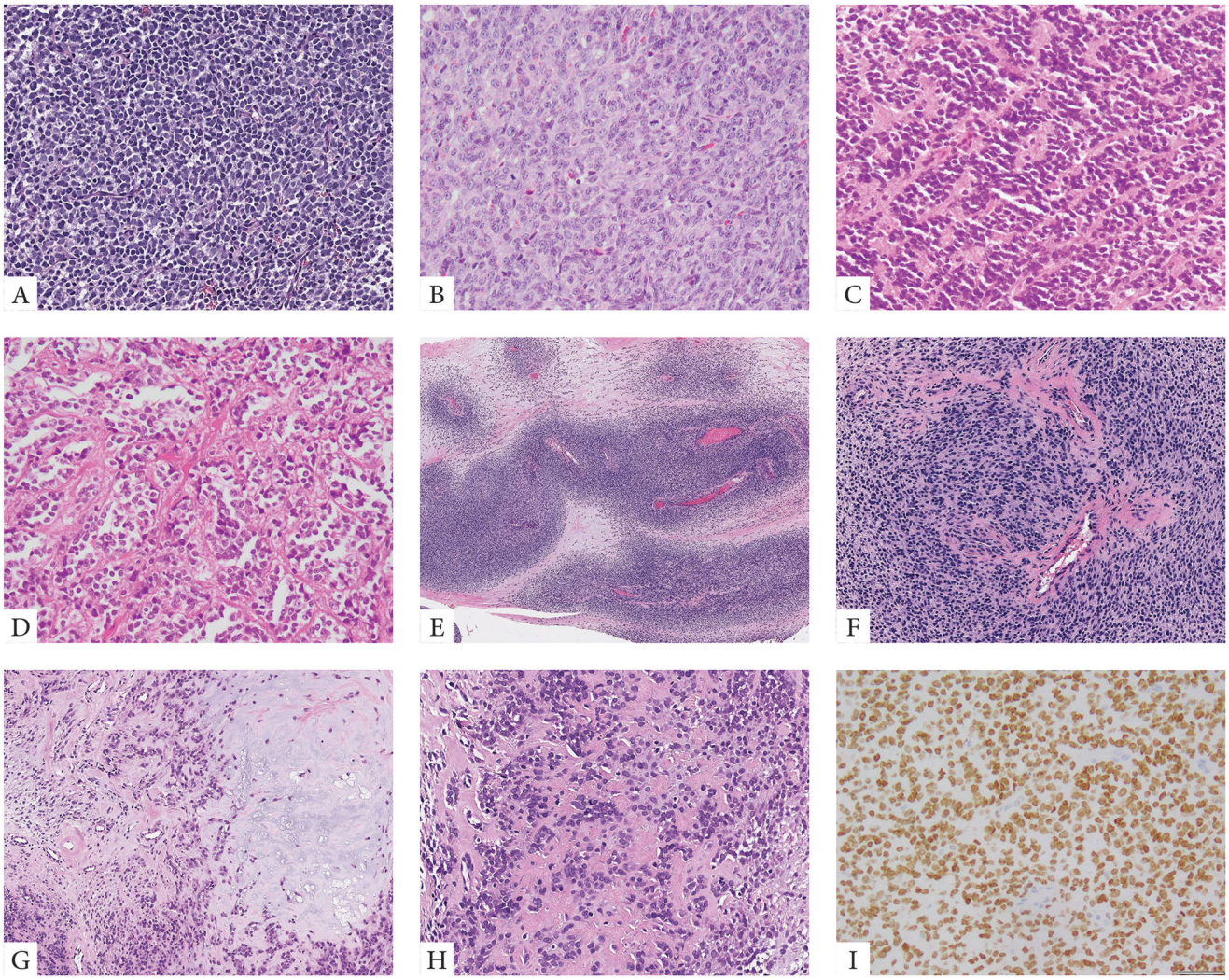

Figure 1. Morphologic spectrum of URCS with *YWHAE* and *BCOR* ITD genetic alterations.

YWHAE-NUTM2B/E positive congenital tumor composed of primitive round cells arranged in solid sheets and vague nests (A, case 4). BCOR-ITD infantile URCS showing a solid growth of undifferentiated round to ovoid cells with scant eosinophilic cytoplasm and vesicular nuclei with small nucleoli, mitotic activity is brisk (B, case 9). Alternative growth patterns included rosette formation and alveolar growth (C, D, case 12). Two cases occurred in adolescents both showing matrix formation radiographically and focally microscopically, being misinterpreted as small cell osteosarcomas (E-H, cases 19&20). The scapular bone lesion in a 16 year-old male showed a marbled appearance on low power with alternating hyper and hypocellular areas (E, case 19); at high power the primitive round cells showed a vague nesting growth and focal hyalinized stroma which in the context of SATB2 positivity was interpreted as osteoid production (F). Similarly, the paraspinal lesion showing vertebral bone involvement and marked sclerosis on radiology, was composed of primitive round cells embedded in a myxochondroid and fibrotic matrix (G, H, case 20). Strong and diffuse BCOR expression is typically seen in all cases (I).

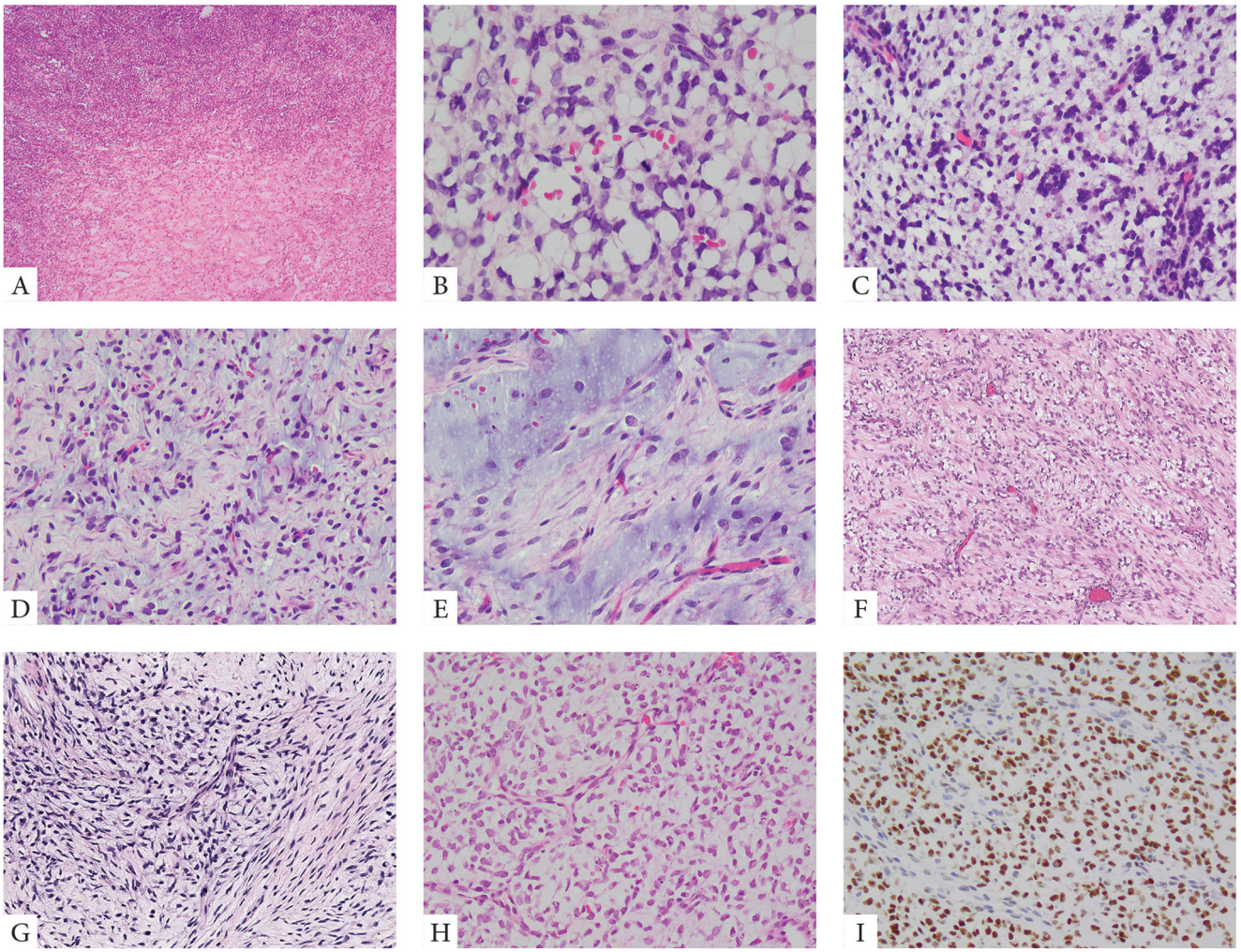

Figure 2. Morphologic spectrum of PMMTI with *BCOR* ITD abnormalities.

A small number of PMMTI cases showed areas of a solid round cell component limited to <30% of the mass (A, case 32). Most tumors however were diffusely myxoid with primitive round, ovoid or spindle cells floating within the extracellular matrix and associated with a delicate capillary network (B-E, cases 22,24,29). Despite low cellularity, the mitotic activity was often increased (B, case 29). Focal areas of spindling within a fibromyxoid stroma was also noted focally in some cases (F, G, cases 28,31). Focal PMMTI-like areas were noted in a subset of URCS (H, case 18). Similar to URCS, PMMTI consistently showed strong immunoreactivity for BCOR (I).

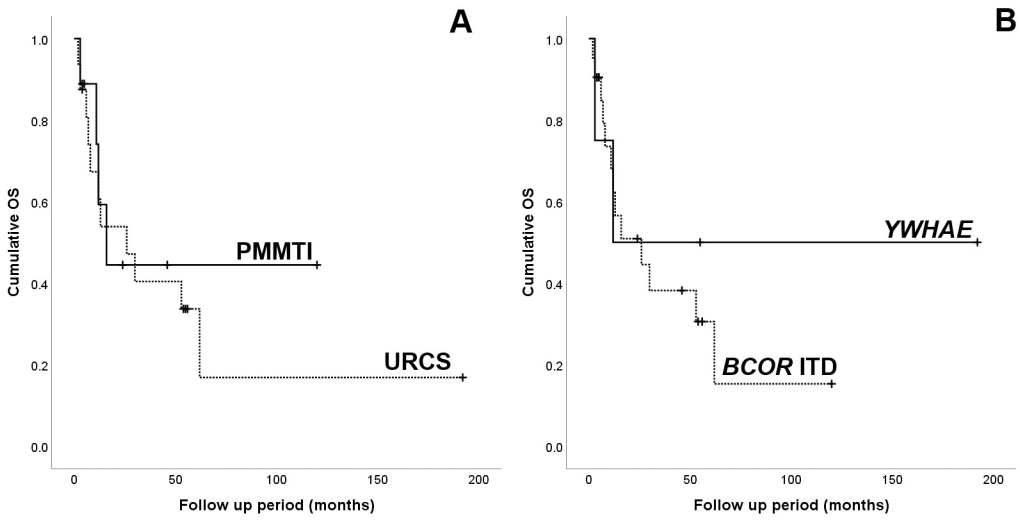

Figure 3.

Kaplan-Meier survival curves showing overall survival for (A) the two histologic types, URCS and PMMTI; and (B) the two genetic abnormalities, *YWHAE* fusions and *BCOR* ITD.

Table 1

Clinicopathologic and molecular findings of *YWHAE-NUTM2B/E* and *BCOR*-ITD positive URCS and PMMTIs

#	Age/Gender	Site	Diagnosis (% myxoid)	Genetics	Follow Up	LR	Mets	Treatment (Surgery -S/Chemotherapy - Ch)
1 *abd	5 mo/F	back	URCS (0%)	*YWHAE-NUTM2B/E*	NED (55 mo)	N	N	S + adjuvant Ch (IVA)
2 *abc	4 mo/M	pelvic	URCS (0%)	*YWHAE-NUTM2B/E*	DOD (3 mo)	N	Y (cerebellum)	S + adjuvant Ch
3 ac	10 mo /M	flank	URCS	*YWHAE-NUTM2B/E*	NED (192 mo)	N	N	neoadjuvant Ch (VACA) >50% necrosis on resection path response
4 a	0 mo/M	buttock/sacral-coccygeal	URCS	*YWHAE-NUTM2B/E*	DOD (12 mo)	N	Y	Ch
5 a	2 mo/F	abd wall	URCS	*YWHAE*	N/A	N/A	N/A	
6 *bd	0 mo/M	back	URCS	*BCOR* ITD (66bp)	DOD (2 mo)	N	N	Ch (VAIA) No response to Ch
7 *bd	0 mo/F	pelvic	URCS (0%)	*BCOR* ITD (66bp)	DOD (26 mo)	Y	Y	Ch (IVA/IVE/IVADo/cisplatin) + S
8 *bd	3 mo/F	jaw	URCS (0%)	*BCOR* ITD (66bp)	DOD (8 mo)	N	N	Ch (VAC) + RT + S
9 *b	11 mo/M	chest wall	URCS (0%)	*BCOR* ITD (96bp)	NED (54 mo)	N	N	S + Ch (VAIA)
10 *bd	5 mo/M	larynx	URCS (5%)	*BCOR* ITD (99bp)	DOD (62 mo)	Y	Y	S + Ch (VA, then ID)
11 *b	5 mo/M	RP/pelvis	URCS (5%)	*BCOR* ITD (n/a)	DOD (30 mo)	Y	N	S + Ch (IVADo) + S
12 *b	10 mo/M	para-vertebral	URCS (0%)	*BCOR* ITD (99bp)	DOD (7 mo)	N	N	S + Ch (IVADo/IVE) + RT
13 b	11 mo/F	pre-sacral	URCS (0%)	*BCOR* ITD (129bp)	DOD (13 mo)	N	Y (multiple brain mets)	Ch (VAC/IE) + S + brachytherapy response to Ch: 90% reduction in tumor size
14 b	6 mo/F	i-abd	URCS (0%)	*BCOR* ITD (n/a)	DOD (53 mo)	Y	N	S + Ch (VAC)
15 b	6 mo/F	abd wall	URCS (10%)	*BCOR* ITD (93bp)	DOD (6 mo)	N	Y (B, ST, L)	Ch
16 b	2/M	abd/pelvic	URCS (0%)	*BCOR* ITD (93bp)	N/A	N/A	N/A	
17 b	19 mo/M	brain, CPA/post fossa	URCS (0%)	*BCOR* ITD (126bp)	AWD (56 mo)	Y	N	S + Ch + RT
18 *bd	0 mo/F	chest wall post med	URCS hyb (10%)	*BCOR* ITD (93bp)	N/A	N/A	N/A	
19 e	16/M	scapula	URCS (0%)	*BCOR* ITD (n/a)	N/A	N/A	N/A	

#	Age/Gender	Site	Diagnosis (% myxoid)	Genetics	Follow Up	LR	Mets	Treatment (Surgery -S/Chemotherapy - Ch)
20[e]	17/M	paraspinal	URCS (10%)	*BCOR* ITD (n/a)	NED (4 mo)	N	N	S + Ch (MAP)
21[b]	11 mo/ F	intracranial extra-axial	PMMTI (90%)	*BCOR* ITD (n/a)	N/A	N/A	N/A	
22[*bd]	2 mo/M	paraspinal	PMMTI (90%)	*BCOR* ITD (96bp)	NED (46 mo)	Y	Y	Ch (VA, then IVA) + S
23[*b]	4 mo/F	para-vertebral	PMMTI (30%)	*BCOR* ITD (120bp)	AWD (120 mo)	Y	Y	S + Ch (VA, the IVA)
24[*b]	9 mo/F	abd wall	PMMTI (90%)	*BCOR* ITD (96bp)	AWD (5 mo)	Y	N	N/A
25[b]	10 mo/M	intra-thoracic	PMMTI (90%)	*BCOR* ITD (96bp)	DOD (16 mo)	Y	Y	S; Ch (ICE) + hyperthermia for recurrence, no path response
26[b]	12 mo/F	ankle	PMMTI (90%)	*BCOR* ITD (96bp)	DOC (11 mo)	Y	Y (tibia, inguinal LN)	
27[*b]	0 mo/M	neck, recurrent	PMMTI (80%)	*BCOR* ITD (66bp)	AWD (4 mo)	Y	N	S + adjuvant Ch
28[e]	12 mo/M	RP/i-abd	PMMTI (90%)	*BCOR* ITD (n/a)	DOD (12 mo)	N	Y	Ch (IVA, VACA, irinotecan, temozolomide)
29[*b]	3 mo/M	RP	PMMTI (90%)	*BCOR* ITD (96bp)	DOD (3 mo)	N	N	Ch (IVADo)
30[b]	12 mo/M	Intraspinal L1-L5	PMMTI (90%)	*BCOR* ITD (96bp)	NED (24 mo)	N	N	S + Ch
31[b]	11 mo/F	orbit	PMMTI (80%)	*BCOR* ITD (96bp)	N/A	N/A	N/A	
32[*b]	6 mo/M	RP/para-vertebral	PMMTI (40%)	*BCOR* ITD (n/a)	N/A	N/A	N/A	
33[*b]	10 mo/F	abd mass	PMMTI (40%)	*BCOR* ITD (63bp)	N/A	N/A	N/A	

[*] 17 cases previously reported[4]

[a] by FISH

[b] by PCR

[c] by conventional karyotype

[d] by whole transcriptome sequencing

[e] targeted NGS sequencing

N/A, not available; RP, retroperitoneum; F, female; M, male; mo, months; abd, abdominal; NED, no evidence of disease; DOD, died of disease; AWD, alive with disease; DOC, died of other causes; LR, local recurrence; Mets, metastasis; Ch, chemotherapy; S, surgery; RT, radiotherapy; VA: vincristine-actinomycin-D; IVA: ifosfamide-vincristine-actinomycin-D; IVE: ifosfamide-vincristine, etoposide; VAIA: vincristine-actinomycin-D-ifosfamide-adriamycin; IVADo: ifosfamide-vincristine-actinomycin-D-doxorubicin; VACA: vincristine-actinomycin-D-cyclophosphamide; VACA: vincristine-actinomycin-D-cyclophosphamide-adriamycin; ID: ifosfamide-doxorubicin; IE: ifosfamide-etoposide; ICE: ifosfamide-carboplatin-etoposide;